







Robust and Real-Time State Estimation of Unstable Microgrids Over IoT Networks

Md. Noor-A-Rahim , Mohammad Omar Khyam, Md. Apel Mahmud , *Senior Member, IEEE*,
Md. Tanvir Ishtaique ul Huque , Xinde Li , *Senior Member, IEEE*, Dirk Pesch , *Senior Member, IEEE*,
and Amanullah M. T. Oo , *Senior Member, IEEE*

Abstract—Smart grid is expected to make use of Internet-of-Things (IoT) networks to reliably monitor its state from remote places. However, due to a potentially unstable nature of a smart grid plant, in particular, when using renewable energy sources, and an unreliable wireless channel used in IoT, it is a challenging task to reliably track the state of smart grids. This article proposes a robust communication framework for state estimation/tracking of unstable microgrids, which is a key component of a smart grid. We present an IoT-integrated smart grid system to monitor the status of microgrids over a wireless network. A delay-universal-based error correction code is utilized to achieve a reliable and real-time estimation of microgrids. To exploit the features of the delay-universal coding scheme, we propose an iterative estimation technique. Through numerical results, we show that the proposed scheme can closely track the state of an unstable microgrid. We also show the impact of wireless network parameters on the estimation performance. The estimation performance of the proposed scheme is compared with the estimation performance of a traditional error correction coding scheme. We show that the proposed scheme substantially outperforms the traditional scheme.

Index Terms—Internet-of-things (IoT), microgrid, smartgrid, real-time estimation and control.

I. INTRODUCTION

THE future of our energy systems is based on the notion of smart grids, which will through the connection and state monitoring of generation and consumption assets through

Manuscript received December 24, 2019; revised May 20, 2020; accepted May 20, 2020. Date of publication June 9, 2020; date of current version June 16, 2021. This work was supported in part by the Science Foundation Ireland, in part by the European Regional Development Fund under Grant 13/RC/2077, in part by the European Unions Horizon 2020 Research and Innovation Programme under the EDGE CO-FUND Marie Skłodowska Curie Grant 713567, in part by the National Natural Science Foundation of China under Grant 61573097 and Grant 91748106, and in part by the Key Laboratory of Integrated Automation of Process Industry under Grant PALN201704. (Corresponding author: Md. Noor-A-Rahim.)

Md. Noor-A-Rahim and Dirk Pesch are with the School of Computer Science and Information Technology, University College Cork, Cork T12 K8AF, Ireland (e-mail: m.rahim@cs.ucc.ie; d.pesch@cs.ucc.ie).

Mohammad Omar Khyam is with the School of Engineering and Technology, Central Queensland University, Melbourne, VIC 3000, Australia (e-mail: m.khyam@cqu.edu.au).

Md. Apel Mahmud and Amanullah M. T. Oo are with the School of Engineering, Deakin University, Geelong, VIC 3217, Australia (e-mail: apel.mahmud@deakin.edu.au; aman.m@deakin.edu.au).

Md. Tanvir Ishtaique ul Huque is with the CyberSecurity Centre, Queensland University of Technology, Brisbane, QLD 4000, Australia (e-mail: tanvir.huque@yahoo.com).

Xinde Li is with the School of Automation, Southeast University, Nanjing 210096, China (e-mail: xindeli@seu.edu.cn).

Digital Object Identifier 10.1109/JSYST.2020.2997065

Internet of Things (IoT) networks allow us to match the required energy exactly to the generated energy [1]. Realizing such a capability will have a transformative impact on many application domains in residential, business, and industrial energy use [2]. Attempts to achieve stable and reliable grid operations for these applications have generally relied on robust and real-time state estimation of generation and consumption assets over an IoT network [3], [4]. However, state estimation in smart grids is challenging as the communication between the smart grid's components, such as a microgrid, and the grid management system is usually accomplished via a wireless link. Therefore, a proper communication and estimation scheme is a prerequisite that is robust in the presence of factors such as noise or fading, which introduce errors into the wireless channel. Significant effort has been made toward state estimation of a smart grid and different algorithms and tools have been proposed in the literature. State estimation techniques can generally be categorized into the following two distinct classes [5].

- 1) Centralized state estimation, where a central state estimation unit collects and processes all measurements from local sensors to obtain a global estimation.
- 2) Distributed state estimation, where every local estimator calculates the state information based on its individual measurements and forwards its estimation to the central state estimation unit.

The former approach demands extensive computational and communication resources and is vulnerable to single-point failure [6]. Consequently, the latter approach is considered as a promising alternative as it not only requires less communication bandwidth but also enables parallel processing. Therefore, a range of state estimation techniques and tools have been developed in previous works. For example, in [7], a hierarchical framework is proposed, where, in the first layer the local state estimation is performed for all subsystems in parallel, and in the second layer, the coordination of these local estimations is realized. However, the proposed hierarchical estimation technique suffers from low reliability. A similar technique has also been studied in [8] and [9] for multiarea power systems. A survey of recent advances in the multiarea state estimation is discussed in [10]. A multilevel framework is proposed in [11], which integrates the existing state estimator that operates at different levels of modeling

hierarchy to monitor large-scale interconnected power systems. As an extension of this idea, in [12], a fully distributed Gauss-Newton iteration scheme for the state estimation of the electric power systems is proposed. Here, at each iteration, a matrix-splitting strategy is used to execute the matrix inversion, as it is required for the Gauss-Newton iteration. Another widely used approach in the smart grid state estimation is the distributed Kalman filter (DKF). For example, in [13], a distributed hierarchical framework for the DKF is proposed where each sensor node independently computes local Kalman filter (KFs), which are then combined by a central processor to calculate the global estimates. A distributed extended and unscented information filters are analyzed in [14] for the condition monitoring of electric power transmission and distribution systems. In [15], a real-time power system state estimation is proposed based on a decentralized unscented KF algorithm. Finally, in [16], using a weighted averaging technique, a DKF is proposed.

Although a considerable amount of research has been carried out toward state estimation in microgrids over the past decade, most of the work assumed that the communication channel is ideal. In other words, most of the literature did not consider the impact of an erroneous communication link between the sensors in a microgrid and the state estimation/monitoring unit with few exceptions [17]–[19]. In [18], the state estimation through wireless sensor networks over fading channels and missing measurements causing packet loss are analyzed using the KF. Moreover, a filtering algorithm is developed in [19] considering the missing measurements to deal with the state estimation in power systems by taking the measurements as inequality constraints. Considering packet losses, in [17], a linear quadratic Gaussian control strategy is developed, which is suitable for the centralized power system state estimation and control. Most of these works assumed a stable smart grid system, which is typically not the case in practice, in particular with renewable energy sources, where the stability margin changes during the practical operation. Moreover, no robust communication framework is developed to tackle the errors generated through unreliable communication links. Thus, despite significant efforts toward developing state estimation techniques for smart grids, the fundamental problem to reliably track the state of smart grids over an IoT network remains to be solved due to the unstable nature of smart grids and the unreliable nature of wireless communication channels used with IoT networks.

In this article, we present a robust communication framework to track the state of an unstable microgrid over IoT networks. For reliable and real-time tracking of the microgrid's state, we utilize a delay-universal coding scheme to mitigate the errors generated by the wireless channel. We propose an iterative estimation technique to exploit some unique features of the delay-universal code. We show that together with the proposed estimation technique, the proposed communication approach can closely track the states of an unstable microgrid. We also investigate the impact of different parameters of the wireless channel on the estimation performance. The performance of the

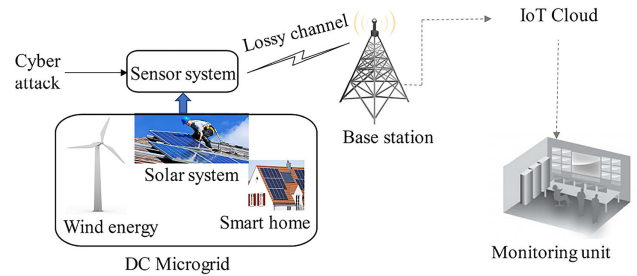


Fig. 1. Monitoring of a dc microgrid via an IoT network.

proposed scheme is compared with that of the traditional communication and estimation approach. Through numerical results, we show that the proposed scheme significantly outperforms the traditional approach in terms of tracking performance.

The remainder of this article is organized as follows. Along with a general system model of an IoT-enabled smart grid, we present the state-space model of the dc microgrid in Section II. The communication framework with delay-universal and traditional coding schemes is described in Section III. In Section IV, we present the proposed iterative estimation technique to exploit the features of the delay-universal code. Along with this comparison, the performance evaluation of the proposed scheme is presented in Section V. Finally, Section VI concludes this article.

II. SMART GRIDS IN IOT NETWORKS

The main theme of the IoT concept is to connect devices over the internet and monitor/access those devices anytime from anywhere. In recent years, the IoT has gained significant attention in the smart grid community, as IoT can be a potential solution to remotely monitor and/or control the smart grid in real time. Especially, the IoT can play a vital role in monitoring/controlling microgrids, which can be considered as a subset of a smart grid. The general framework of an IoT-enabled microgrid monitoring system is shown in Fig. 1. This microgrid contains a smart sensor system, which senses the state of the microgrid and transmits the sensing information to an energy management/monitoring unit. As microgrids are generally located in remote places due to the space requirements of, for example, wind or solar farms, the sensor system communicates with the energy management/monitoring unit via a wireless IoT network. Thus, it is essential to ensure reliable and real-time wireless communication between the sensor system and gateways, e.g., base stations or even satellites. Before presenting a robust communication framework for an IoT-enabled microgrid in the following section, we first present a dynamic state-space model of a microgrid in the following.

A. DC Microgrid in Smart Grids and Its State-Space Model

A dc microgrid, which typically integrates a number of dc sources and dc loads, offers an advantage over ac microgrids in terms of the system efficiency, cost, and system size as it eliminates the redundant energy conversion [20]. In general,

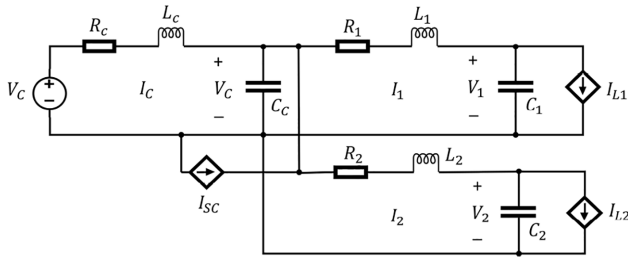


Fig. 2. Simplified equivalent circuit diagram of a dc microgrid.

a dc microgrid consists of the following main components [3], [21].

- 1) *Source*: The renewable energy source is represented by an equivalent dc voltage source.
- 2) *Filters*: A series of line filters are used to reduce the voltage/current harmonics and electromagnetic interferences.
- 3) *Loads*: Motor-type dc loads along with the battery and resistive loads are generally used in dc microgrids.

Fig. 2 shows a simplified equivalent circuit diagram of a dc microgrid, where R , L , C , I , and V are the resistance, inductance, capacitance, current, and voltage, respectively, whereas the subscripts c , 1, 2, sc , $L1$, and $L2$ represent the component of converter, filter 1, filter 2, supercapacitor, load 1, and load 2, respectively. From Fig. 2, the differential equations of the microgrid can be derived as follows by applying Kirchhoffs laws [22] as

$$\begin{aligned}\Delta I_c(k+1) &= \frac{-R_c \Delta I_c(k) - \Delta V_c(k)}{L_c} \\ \Delta I_1(k+1) &= \frac{-R_1 \Delta I_1(k) + \Delta V_c(k) - \Delta V_1(k)}{L_1} \\ \Delta I_2(k+1) &= \frac{-R_2 \Delta I_2(k) + \Delta V_c(k) - \Delta V_2(k)}{L_2} \\ \Delta V_c(k+1) &= \frac{\Delta I_c(k) - \Delta I_1(k) - \Delta I_2(k) + \Delta I_{sc}(k)}{C_c} \\ \Delta V_1(k+1) &= \frac{\Delta I_1(k) + \Delta I_{L1}(k)}{C_1} \\ \Delta V_2(k+1) &= \frac{\Delta I_2(k) + \Delta I_{L2}(k)}{C_2}\end{aligned}$$

where Δ in the aforementioned equations denotes the deviation of the system state variables around the operating points. At any time step k , the aforementioned partial differential equations representing the microgrid can be written in the following discrete system dynamic form:

$$\mathbf{X}_{k+1} = \mathbf{A}\mathbf{X}_k + \mathbf{B}\mathbf{U}_k + \mathbf{w}_k \quad (1)$$

where \mathbf{X} is the state of the microgrid defined by $\mathbf{X} = [\Delta I_c \ \Delta I_1 \ \Delta I_2 \ \Delta V_c \ \Delta V_1 \ \Delta V_2]$; \mathbf{U} is the control input defined by $\mathbf{U} = [\Delta I_{sc} \ \Delta I_{L1} \ \Delta I_{L2}]$; \mathbf{w} is bounded noise/disturbance with $\mathbf{w} \in \{W^-, W^+\}$; \mathbf{A} is a discretized state matrix defined by $\mathbf{A} = \mathbf{I} + \alpha \delta t$, where α is given in (2) and δt is the discretization step size; and \mathbf{B} is the control distribution matrix defined by

$\mathbf{B} = \mathbf{I} + \beta \delta t$, where β is given in (3).

$$\alpha = \begin{bmatrix} -\frac{R_c}{L_c} & 0 & 0 & -\frac{1}{L_c} & 0 & 0 \\ 0 & -\frac{R_1}{L_1} & 0 & \frac{1}{L_1} & -\frac{1}{L_1} & 0 \\ 0 & 0 & -\frac{R_2}{L_2} & \frac{1}{L_2} & 0 & -\frac{1}{L_2} \\ \frac{1}{C_c} & -\frac{1}{C_c} & -\frac{1}{C_c} & 0 & 0 & 0 \\ 0 & \frac{1}{C_1} & 0 & 0 & 0 & 0 \\ 0 & 0 & \frac{1}{C_2} & 0 & 0 & 0 \end{bmatrix} \quad (2)$$

$$\beta^T = \begin{bmatrix} 0 & 0 & 0 & \frac{1}{C_c} & 0 & 0 \\ 0 & \frac{1}{C_1} & 0 & 0 & \frac{1}{C_1} & 0 \\ 0 & 0 & \frac{1}{C_2} & 0 & 0 & \frac{1}{C_2} \end{bmatrix}. \quad (3)$$

In the rest of the article, we consider the control input $\mathbf{U} = \mathbf{0}$ for the sake of simplicity, as the main focus of this article is to track the state of the microgrid rather than the control. With the aforementioned specifications of the microgrid, it can be shown that the microgrids are unstable, i.e., $|\mathbf{A}| > 1$. Thus, with a high probability, it can be shown that the state of the microgrid will grow unbounded with the progression of time. However, a limited rate communication link is not sufficient to encode and transmit the unbounded state. Thanks to the bounded noise, we can estimate the state by knowing the noise provided that the initial state is known [23]. In the following section, we present the communication approach to transmit the bounded noise and perform the estimation based on the observed bounded noise at the receiver.

III. PROPOSED COMMUNICATION STRATEGY

A microgrid can be monitored remotely by leveraging a wireless communication technique. However, due to the uncertainty in the wireless network, a robust communication framework is required to tackle the error induced from the wireless channel. In the following, we present the proposed communication framework to monitor the state of the microgrid over a wireless network. As mentioned in the previous section, due to the unstable nature of the microgrid, it is not feasible to quantize and encode the actual state of the microgrid. As the process noise is bounded, we quantize, encode, and transmit the bounded noise instead of the actual state. In practice, it may not be feasible to sample and transmit the observed microgrid's states at every time interval δt (especially when δt is very small) due to hardware constraints.

Let τ be the number of discrete time steps after which the sensor system of the microgrid performs sampling and transmission. In other words, the states of the microgrid are sampled at time step $k = 0, \tau, 2\tau, \dots$. Considering sampling interval and all zero control input, the equivalent dynamic system of (1) can be written as

$$\mathbf{X}_s = \mathbf{A}^\tau \mathbf{X}_{s-1} + \mathbf{v}_s \quad (4)$$

where s is the sampling instant defined in discrete-time step $k = s\tau$ and \mathbf{v}_s is the accumulated noise defined by $\mathbf{v}_s = \sum_{j=0}^{\tau-1} \mathbf{A}^{\tau-1-j} \mathbf{w}_{s+j}$. Since \mathbf{w}_k is bounded, \mathbf{v}_s will also be bounded. Hence, at every time interval of $\tau \delta t$, the sensor system

samples and transmits the accumulated noise. The details of sampling and transmission processes are given later.

At any sampling instant i , the transmitter of the sensor system performs the uniform quantization on each element of ν_i and transforms each element to ℓ_q bits. We combine those bits and form a bit block $\mathbf{b}_i = [b_{i1}, b_{i2}, \dots, b_{i\ell_b}]$, where $\ell_b = n \cdot \ell_q$ and n is the number of elements in ν_i . We apply a ℓ_r -bits cyclic redundancy check (CRC) code on \mathbf{b}_i to detect errors at the receiver. By merging the CRC coded resultant bits $\mathbf{r}_i = [r_{i1}, r_{i2}, \dots, r_{i\ell_r}]$, we form $\mathbf{m}_i = [\mathbf{b}_i \mathbf{r}_i] = [m_{i1}, m_{i2}, \dots, m_{i\ell_m}]$, where $\ell_m = \ell_b + \ell_r$. To correct the error induced by the wireless channel, we apply error correction codes on \mathbf{m}_i and produce a ℓ_c -bits code word $\mathbf{c}_i = [c_{i1}, c_{i2}, \dots, c_{i\ell_c}]$ with $\ell_c = \frac{\ell_m}{\rho_c}$, where ρ_c is the rate of the error correction code. In this article, we investigate the estimation performance by considering two different error correction codes, which will be discussed in the following subsections. We perform modulation on \mathbf{c}_i and transmit the modulated signal. In this article, we perform binary phase shift keying (BPSK) on \mathbf{c}_i and produce $\mathbf{x}_i = [x_{i1}, x_{i2}, \dots, x_{i\ell_c}]$. The received signal corresponds to the j th modulated symbol is given by

$$y_{ij} = x_{ij} + \kappa \quad (5)$$

where κ is the additive white Gaussian noise with standard deviation (s.d.) σ . Upon receiving the signal $\mathbf{y}_i = [y_{i1}, y_{i2}, \dots, y_{i\ell_c}]$, the receiver performs the reverse process to reconstruct the estimated version of ν_i . In other words, the receiver performs the following operations sequentially, e.g., demodulation, decoding, CRC checking, and dequantization. Based on the estimated noise, the receiver estimates the current state of the microgrid. Details of the estimation technique are discussed in the next section.

To encode \mathbf{b}_i , we consider the following two error correction coding strategies: traditional block coding and delay-universal coding. For the traditional block coding strategy, we consider a traditional repeat accumulate (RA) code [24], while for the delay-universal coding strategy, we consider a limited memory delay-universal code [25], which is built on the regular RA code. Both codes are described in the following subsections.

A. Repeat Accumulate (RA) Code

The RA code is a class of low-density parity-check (LDPC) codes [26] that exhibits asymptotically capacity approaching error correction performance, while offering low encoding and decoding complexities [24]. The RA codes can be represented by a connected bipartite graph, which consists of ℓ_c variable nodes and ℓ_p check nodes. Variable nodes are further divided into two types, namely message nodes and parity nodes of quantity of ℓ_m and ℓ_p , respectively, such that $\ell_c = \ell_m + \ell_p$. The code rate of the RA code is defined by $\rho_c = \frac{\ell_m}{\ell_c}$. Each of the message nodes, which represents each of the bits of \mathbf{m}_i , is connected with one or more check nodes. Each of the parity nodes, which represents each of the bits of \mathbf{p}_i , is connected with two consecutive check nodes. Essentially, each of the check nodes satisfies that the modulo-2 sum of all connecting variable nodes is zero. Note that

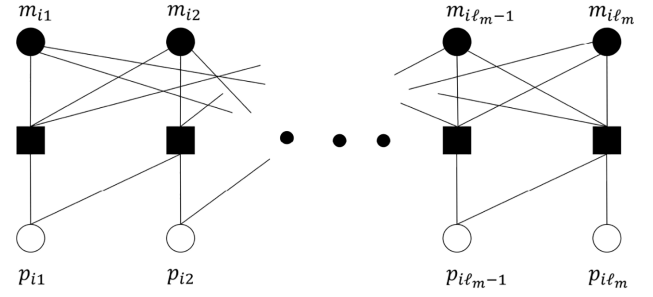


Fig. 3. Rate $\frac{1}{2}$ regular RA code with $(d_m, d_c) = (3, 3)$. In the figure, circles and squares represent variable and check nodes, respectively. Among the circles, filled circles represent message nodes, while empty circles represent parity nodes.

the number of connections with each node is called the degree of that node. An RA code is called a regular (d_m, d_c) -RA code, if every message node and check node have exactly d_m and d_c degrees, respectively. An example of a $(d_m, d_c) = (3, 3)$ -regular rate- $\frac{1}{2}$ RA code is shown in Fig. 3.

Encoding: Due to the systematic nature of the RA code, the message bits (i.e., \mathbf{m}_i) are embedded in the encoded output. More precisely, the code word \mathbf{c}_i is formed by $\mathbf{c}_i = [m_{i1}, m_{i2}, \dots, m_{i\ell_m}, p_{i1}, p_{i2}, \dots, p_{i\ell_p}]$. The value of the j th parity node (i.e., p_{ij}) is determined by the modulo-2 sum of $p_{i(j-1)}$ and all the message nodes connected to the j th check node.

Decoding: RA code words can be decoded via message passing iterative decoding [27], which offers good decoding performance with low decoding complexity. As the name suggests these algorithms are associated with passing messages from variable nodes to check nodes and from check nodes to variable nodes. The belief propagation algorithm is one of the most prominent categories of message passing algorithms. In the belief propagation algorithm, the messages passed between the nodes are expressed as log-likelihood ratios (LLRs). For a j th code word bit, the LLR obtained from the channel is given by

$$\gamma_j = \log \frac{P_{ch}(c_j = 0|y_j)}{P_{ch}(c_j = 1|y_j)} \quad (6)$$

where $P_{ch}(c_j = 0|y_j)$ and $P_{ch}(c_j = 1|y_j)$ represent the probabilities that c_j is 0 and 1, respectively, when the channel output is y_j . Let $\Gamma_c^{(\eta)}(v, u)$ be the outgoing LLR value from the check node v to variable node u at iteration η , which is calculated by [27]

$$\Gamma_c^{(\eta)}(v, u) = 2 \tanh^{-1} \left(\prod_{u' \in \mathcal{S}_v(v), u' \neq u} \tanh \left(\frac{\Gamma_v^{(\eta)}(v, u')}{2} \right) \right) \quad (7)$$

where $\Gamma_v^{(\eta)}(v, u)$ be the outgoing LLR value from the variable node v to check node u at iteration η , and $\mathcal{S}_v(u)$ is the set of variable nodes that are connected with the u th check node. Initially, we set $\Gamma_v^{(\eta)}(v, \cdot) = \gamma_j$ and $\Gamma_v^{(\eta)}(v, u)$ is updated by the

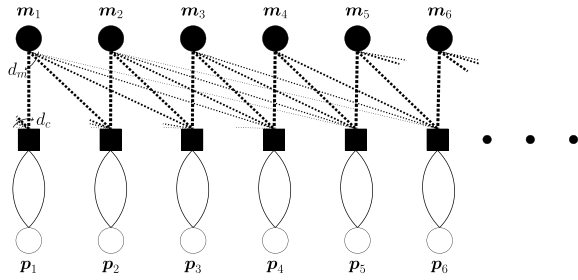


Fig. 4. Delay-universal code based on the regular RA code. The connection probability between message node and check nodes are depicted via thickness of the connected links, where higher thickness refers to higher connection probability.

following equation:

$$\Gamma_v^{(\eta+1)}(v, u) = \sum_{v' \in \mathcal{S}_c(u), v' \neq v} \Gamma_c^{(\eta)}(v', u) + \gamma_u \quad (8)$$

where $\mathcal{S}_c(u)$ is the set of the check nodes that are connected with the u th variable node. The aforementioned algorithm is also known as the sum-product algorithm due to the sum and product operations in (7) and (8), respectively. After a predefined maximum iteration η_{\max} , the u th decoded bit is determined by

$$\hat{c}_u = \begin{cases} 0, & \text{if } \sum_{n \in \mathcal{S}_c(u)} \Gamma_c^{(\eta_{\max})}(v, u) + r_u \geq 0 \\ 1, & \text{if } \sum_{n \in \mathcal{S}_c(u)} \Gamma_c^{(\eta_{\max})}(v, u) + r_u < 0. \end{cases} \quad (9)$$

B. Delay-Universal Code Based on RA Code

Delay-universal codes (also known as anytime codes) are shown to be suitable for tracking and controlling an unstable plant over a noisy channel. A delay-universal code needs to have the following communication requirements: causal encoding, real-time decoding, and exponential decay of error probability for a given code word. In this article, we construct the delay-universal code by coupling the RA protographs (regular RA code of small size). We construct the delay-universal code in the following two steps:

- 1) by coupling standard (d_m, d_c) -regular RA protographs such that each of the d_m edges of a message node at the position j is connected to the check nodes at positions j to $j + \psi$, where $\psi \gg d_m$ is the coupling length and the connection probability follows an exponential distribution;
- 2) by lifting and permuting the coupled protographs.

We consider ℓ_m as the lifting factor, i.e., each position/protograph contains ℓ_m message nodes, $\frac{d_m}{d_c} \ell_m$ check, and parity nodes. Thus, the message and parity nodes at the position i represent \mathbf{m}_i and \mathbf{p}_i , respectively. A delay-universal code obtained from coupled RA protographs is shown in Fig. 4.

Encoding: The previously described delay-universal code offers similar systematic encoding to that of the traditional RA code. However, unlike the traditional RA code where the generated parity bit block (for example, \mathbf{p}_i) solely depends on the current message bit block (i.e., \mathbf{m}_i), the delay-universal code produces parity bits based on the current and previous

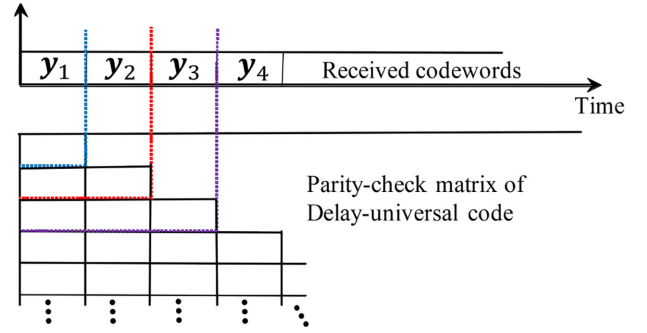


Fig. 5. Expanding window decoding of the delay-universal code.

$\psi - 1$ message bit blocks. For example, a parity bit block \mathbf{p}_i results from the following encoding function $\mathbf{p}_i = f_e(\mathbf{m}_i, \mathbf{m}_{i-1}, \dots, \mathbf{m}_{i-\psi})$. The encoding function performs the modulo-2 sum of previous parity bit and all the message nodes connected to the corresponding check node.

Decoding: The standard belief propagation decoding can be applied to the decoding of the delay-universal code. In other words, (6)–(9) can be used to decode the delay-universal code. However, unlike the decoding of the traditional code where only the received code word is fed into the decoder, the decoder in the delay-universal code takes all the received code words as input, and then, decodes all the received code words. Thus, the decoding process of the delay-universal code is like an expanding window decoder, where the decoding window expands at every time instant by including the received code word. An expanding window decoder for the delay-universal code is shown in Fig. 5.

IV. PROPOSED STATE ESTIMATION TECHNIQUE

A. State Estimation With the RA Code

The state estimation technique with the traditional RA code is straightforward. Let $\epsilon_i \in \{0, 1\}$ be the CRC decoded output of message \mathbf{m}_i , where 0 indicates no error in the decoded code word that contains \mathbf{m}_i and 1 indicates otherwise. Let $\hat{\nu}_s$ and $\hat{\mathbf{X}}_s$ be the estimated version of ν_s and \mathbf{X}_s , respectively, at the receiver. With the RA code, the estimated state is given by

$$\hat{\mathbf{X}}_s = \begin{cases} A^\tau \hat{\mathbf{X}}_{s-1} + \hat{\nu}_{s-1}, & \text{if } \epsilon_{s-1} = 0 \\ A^\tau \hat{\mathbf{X}}_{s-1}, & \text{otherwise.} \end{cases} \quad (10)$$

Let d be the time steps required to transmit the bits from the microgrid's sensor system, which is defined by $d = \frac{\ell_{tb}}{D_R \delta t}$, where D_R is the data rate [bits per seconds (bps)] of the communication link and ℓ_{tb} is the total number of bits transmitted from the sensor system at every sample interval. Considering the transmission delay, the estimation of the current state is given by

$$\hat{\mathbf{X}}_{s+d} = A^d \hat{\mathbf{X}}_s. \quad (11)$$

B. Iterative State Estimation With Delay-Universal Code

For the delay-universal code, we propose an iterative state estimation technique. As discussed in the earlier section, the

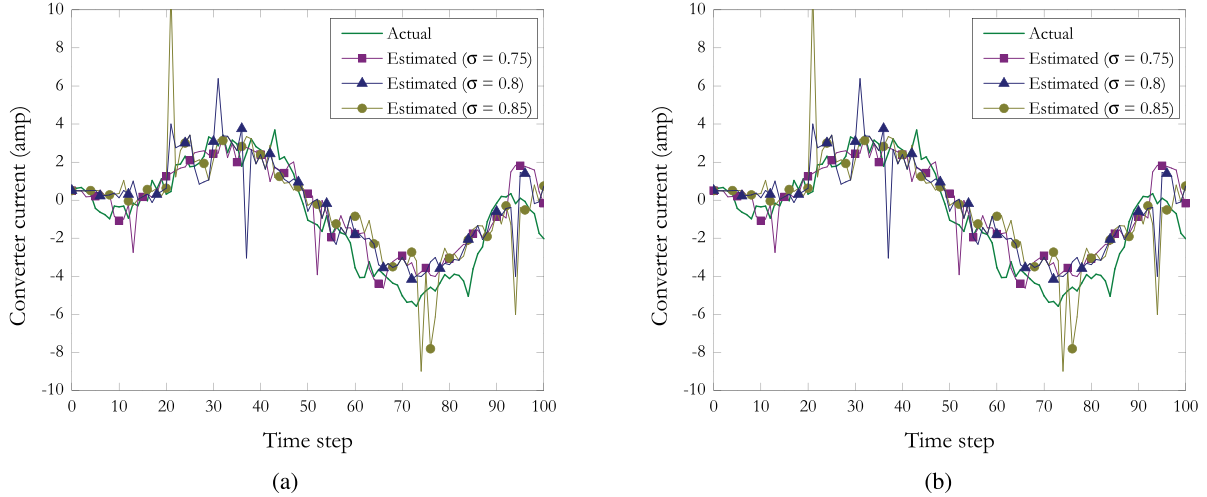


Fig. 6. Estimation performance of the proposed scheme while varying the channel noise. (a) Estimation of converter's current I_c . (b) Estimation of filter 1's current I_1 .

Algorithm 1: Proposed iterative State Estimation Algorithm.

```

1 /* Upon receiving the signal at sampling
   instant  $s$ , we update the estimation of all
   the previous states */
2 for  $j = 1, 2, \dots, s-1$  do
3   if  $\epsilon_j(s) = 0$  then
4      $\hat{\mathbf{X}}_j(s) = A^T \hat{\mathbf{X}}_{j-1}(s) + \hat{\nu}_{j-1}(s)$ 
5   else
6      $\hat{\mathbf{X}}_j(s) = A^T \hat{\mathbf{X}}_{j-1}(s)$ 
7 /* Once we have the updated estimation of the
   previous states, we estimate the state at
   sampling instant  $s$  */
8 if  $\epsilon_s(s) = 0$  then
9    $\hat{\mathbf{X}}_s(s) = A^T \hat{\mathbf{X}}_{s-1}(s) + \hat{\nu}_{s-1}(s)$ 
10 else
11    $\hat{\mathbf{X}}_s(s) = A^T \hat{\mathbf{X}}_{s-1}(s)$ 
12 /* With transmission delay, we estimate the
   current state. */
13  $\hat{\mathbf{X}}_{s+d} = A^d \hat{\mathbf{X}}_s(s)$ 

```

delay-universal code allows us to correct the errors in the current as well as all the previously received code words. By exploiting this characteristic, upon receiving the current message (corresponds to current accumulated noise), we re-decode all the previously received messages (corresponds to previously accumulated noises). Based on the updated accumulated noises, we also update the estimation of all the previous states. Then, the current state is calculated from the updated previous states and the current accumulated noise. The summary of the proposed iterative state estimation technique is presented in Algorithm 1. The notations used in the algorithm are defined in the following:

- 1) $\hat{\nu}_i(s)$ is the estimation of ν_i at the sampling instant s ;
- 2) $\epsilon_i(s)$ indicates error in decoded codeword i at the sampling instant s ;
- 3) $\hat{\mathbf{X}}_i(s)$ is the estimation of \mathbf{X}_i at the sampling instant s . Hence, $\hat{\mathbf{X}}_s(s)$ is the estimation at the current sampling instant.

TABLE I
STATE SPACE PARAMETERS

| Parameters | Value | Description. |
|------------|---------------------------------|--------------------------|
| R_c | 0.4Ω | Resistances of converter |
| R_1 | 0.8Ω | Resistances of filter 1 |
| R_2 | 0.42Ω | Resistances of filter 2 |
| C_c | $1050 \times 10^{-6} \text{ F}$ | Capacitance of converter |
| C_1 | $200 \times 10^{-6} \text{ F}$ | Capacitance of filter 1 |
| C_2 | $1050 \times 10^{-6} \text{ F}$ | Capacitance of filter 2 |
| L_c | $17.3 \times 10^{-3} \text{ H}$ | Inductance of converter |
| L_1 | $20 \times 10^{-3} \text{ H}$ | Inductance of filter 1 |
| L_2 | $19.6 \times 10^{-3} \text{ H}$ | Inductance of filter 2 |

V. RESULTS AND DISCUSSIONS

In this section, we present the performance evaluation of the proposed communication frameworks by tracking the state of the microgrid. The state-space parameters used in the simulation are given in Table I. The parameters are chosen from the experimental setup presented in [21]. The discretization step δt is set to 0.0002 s. With this setup, we notice that $A > 1$, i.e., the microgrid plant is unstable. We consider a 6-bit uniform quantizer to quantize and transform the observed noise to binary bits. For the CRC encoding, we consider a 4-bits CRC code, specified by the polynomial $x^4 + x + 1$, which is one used in many ITU-T standards. As the number of elements in the observed microgrid's state is six, the length of m_i becomes $\ell_m = 40$. We construct the delay-universal code from a chain of $(d_m, d_c) = (4, 4)$ rate $\frac{1}{2}$ RA protographs with $\psi = 10$. Thus, the length of each encoded message c_i becomes $\ell_c = 80$.

For performance evaluation of the proposed (delay-universal) scheme, we first consider a special case where the sensor system samples the observation at every δt interval, i.e., $s = k$. We also assume a very high-speed communication link that allows us to neglect the transmission delay d . In Fig. 6, we present the performance of the proposed communication and estimation technique while tracking the currents of the converter and filter 1. We observe that the proposed scheme can closely estimate

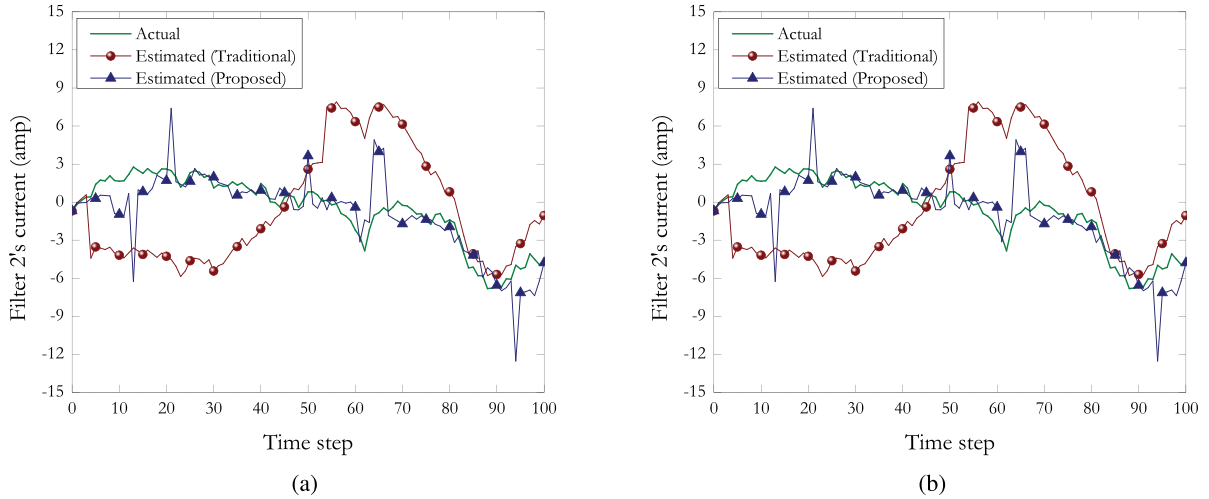


Fig. 7. Comparison of the estimation performance between the proposed and traditional scheme. (a) Estimation of filter 2's current I_2 . (b) Estimation of converter's voltage V_c .

the currents over the noisy communication channel. We also show the impact of the wireless channel's noise on the tracking performance. We observe that the channel noise does not have a significant impact on the tracking performance, while a slight performance degradation is observed with increasing channel noise. In Fig. 7, we present a tracking performance comparison between the traditional regular RA code and the proposed delay-universal code. For fair comparison, we consider a $(d_m, d_c) = (4, 4)$ -regular RA code for the traditional RA code. We show the estimation of filter 2's current and converter's voltage over the wireless channel with noise s.d. $\sigma = 0.8$. We observe that the proposed scheme significantly outperforms the traditional scheme, where the traditional scheme fails to track the state in most of the time steps. With the proposed scheme, the decoded error of previously received messages decays as time progresses. On the other hand, with the traditional RA code, the decoding error of a message does not change over time. Fig. 8 shows the decoding error characteristics of the delay-universal code and traditional RA code with two different channel noises. As expected, we observe that the decoding error gets fixed for the traditional RA code where higher decoding error with larger channel noise. Compared to the traditional scenario, although higher decoding error is initially observed for the proposed scenario, the decoding error decays close to zero as delay increases. Note that the nonzero decoding errors, observed for both channel noises, result from the quantization error.

Now we consider a limited rate communication link with sampling interval larger than δt . We assume the data rate of the communication link is 250 kb/s and set $\tau = 10$, i.e., the sensor system samples and transmits its disturbance observation at every 0.002 s. Along with the 80 encoded bits c_i , we consider 20 bits as header/overhead, which gives a data packet of 100 bits at each transmission. Thus, the transmission time becomes $d = 0.0004$. The estimation performance of the proposed and traditional schemes are shown in Fig. 9. We observe

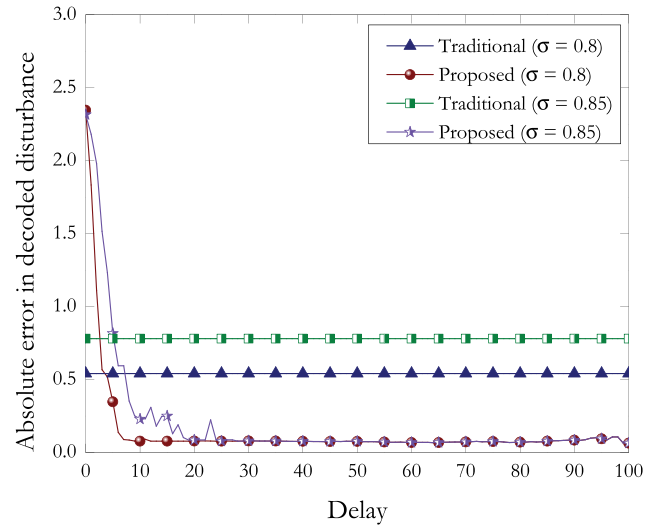


Fig. 8. Decoded error characteristics of the transmitted noise with respect to delay.

that although initially, both schemes exhibit similar performance, the proposed scheme significantly outperforms the traditional scheme with the increase of sampling instant. With the traditional RA code, decoding errors propagate in the subsequent estimations, and hence, we observe a growing estimation error as the time progresses. On the other hand, the delay-universal code can rectify the decoding error propagation by correcting the previous stages errors. In Fig. 10, we present the impact of the data rate of the communication link on the estimation error. We present the absolute estimation error for 250 and 125 kb/s. The transmission time for the later data rate is larger than the former one. As larger transmission time may result in larger variations in accumulated noises, we observe that the estimation error with data rate 125 kb/s is slightly worse than that of 250 kb/s.

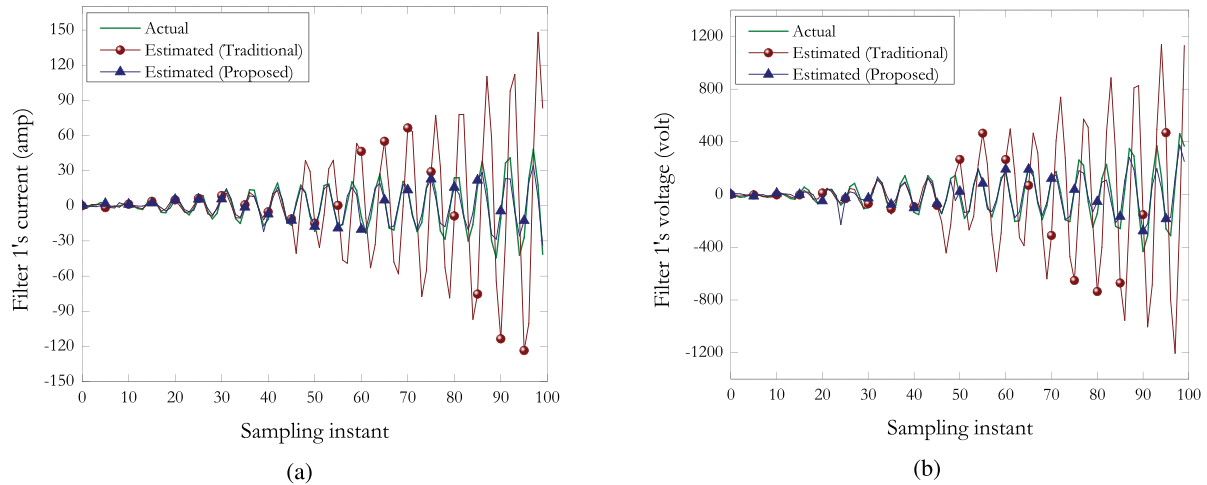


Fig. 9. Comparison of the estimation performance between the proposed and traditional scheme with limited rate communication link. (a) Estimation of filter 2's current I_2 . (b) Estimation of converter's voltage V_c .

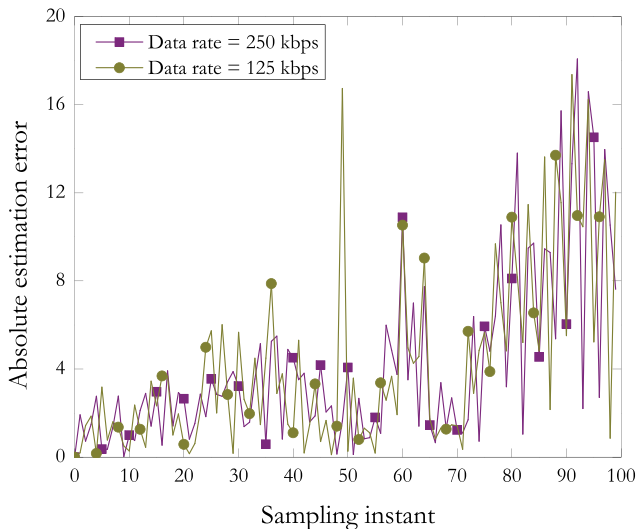


Fig. 10. Impact of data rate of the communication link on the estimation performance.

VI. CONCLUSION

In this article, we have studied the state estimation of a smart grids over an unreliable wireless network. A wireless IoT network integrated communication framework is presented to monitor the state of an unstable microgrid, which is an essential part of a smart grid. To mitigate the error induced by the wireless channel, we have proposed a delay-universal coding scheme in the communication framework. An iterative estimation approach is proposed to exploit the unique features of the delay-universal coding scheme. Through numerical results, we have shown that the proposed communication scheme (along with the proposed estimation technique) is able to closely monitor the state of any unstable microgrid. We have numerically evaluated the impact of the wireless network's parameters on the tracking performances. We have also compared the performance of the

proposed scheme with the performance of a traditional block coding scheme. We have shown that the traditional approach is not sufficient to track the unstable microgrid and the proposed scheme substantially outperforms the traditional approach in terms of tracking performance.

REFERENCES

- [1] L. Yu, T. Jiang, Y. Cao, and Q. Qi, "Carbon-aware energy cost minimization for distributed internet data centers in smart microgrids," *IEEE Internet Things J.*, vol. 1, no. 3, pp. 255–264, Jun. 2014.
- [2] Y. Saleem, N. Crespi, M. H. Rehmani, and R. Copeland, "Internet of things-aided smart grid: technologies, architectures, applications, prototypes, and future research directions," *IEEE Access*, vol. 7, pp. 62 962–63 003, 2019.
- [3] M. M. Rana, W. Xiang, and E. Wang, "Smart grid state estimation and stabilisation," *Int. J. Elect. Power Energy Syst.*, vol. 102, pp. 152–159, Nov. 2018.
- [4] M. Noor-A-Rahim, M. Khyam, X. Li, and D. Pesch, "Sensor fusion and State estimation of IoT enabled wind energy conversion system," *Sensors*, vol. 19, no. 7, p. 1566, Apr. 2019.
- [5] M. H. Cintuglu and D. Ishchenko, "Secure distributed state estimation for networked microgrids," *IEEE Internet Things J.*, vol. 6, no. 5, pp. 8046–8055, Oct. 2019.
- [6] L. Xie, D.-H. Choi, S. Kar, and H. V. Poor, "Fully distributed state estimation for wide-area monitoring systems," *IEEE Trans. Smart Grid*, vol. 3, no. 3, pp. 1154–1169, Sep. 2012.
- [7] T. Van Cutsem, J. L. Howard, and M. Ribbens-Pavella, "A two-level static state estimator for electric power systems," *IEEE Trans. Power App. Syst.*, vol. PAS-100, no. 8, pp. 3722–3732, Aug. 1981.
- [8] T. Yang, H. Sun, and A. Bose, "Transition to a two-level linear state estimator-Part I: Architecture," *IEEE Trans. Power Syst.*, vol. 26, no. 1, pp. 46–53, Feb. 2011.
- [9] T. Yang, H. Sun, and A. Bose, "Transition to a two-level linear state estimator; Part II: Algorithm," *IEEE Trans. Power Syst.*, vol. 26, no. 1, pp. 54–62, Feb. 2011.
- [10] A. Gomez-Exposito, A. Abur, A. de la Villa Jaen, and C. Gomez-Quiles, "A multilevel state estimation paradigm for smart grids," *Proc. IEEE*, vol. 99, no. 6, pp. 952–976, Jun. 2011.
- [11] G. N. Korres, "A distributed multiarea state estimation," *IEEE Trans. Power Syst.*, vol. 26, no. 1, pp. 73–84, 2010.
- [12] A. Minot, Y. M. Lu, and N. Li, "A distributed Gauss-Newton method for power system state estimation," *IEEE Trans. Power Syst.*, vol. 31, no. 5, pp. 3804–3815, Nov. 2015.
- [13] H. R. Hashemipour, S. Roy, and A. J. Laub, "Decentralized structures for parallel Kalman filtering," *IEEE Trans. Autom. Control*, vol. 33, no. 1, pp. 88–94, Jan. 1988.

- [14] G. Rigatos, P. Siano, and N. Zervos, "A distributed state estimation approach to condition monitoring of nonlinear electric power systems," *Asian J. Control*, vol. 15, no. 3, pp. 849–860, 2013.
- [15] A. K. Singh and B. C. Pal, "Decentralized dynamic state estimation in power systems using unscented transformation," *IEEE Trans. Power Syst.*, vol. 29, no. 2, pp. 794–804, Sep. 2013.
- [16] P. Alriksson and A. Rantzer, "Distributed Kalman filtering using weighted averaging," in *Proc. 17th Int. Symp. Math. Theory Netw. Syst.*, 2006, pp. 2445–2450.
- [17] A. K. Singh, R. Singh, and B. C. Pal, "Stability analysis of networked control in smart grids," *IEEE Trans. Smart Grid*, vol. 6, no. 1, pp. 381–390, May 2014.
- [18] D. E. Quevedo and A. Ahlén, "A predictive power control scheme for energy efficient state estimation via wireless sensor networks," in *Proc. IEEE 47th Conf. Decis. Control*, 2008, pp. 1103–1108.
- [19] L. Hu, Z. Wang, I. Rahman, and X. Liu, "A constrained optimization approach to dynamic state estimation for power systems including PMU and missing measurements," *IEEE Trans. Control Syst. Technol.*, vol. 24, no. 2, pp. 703–710, Jul. 2015.
- [20] M. Karbalaye Zadeh, R. Gavagsaz-Ghoachani, S. Pierfederici, B. Nahid-Mobarakeh, and M. Molinas, "Stability analysis and dynamic performance evaluation of a power electronics-based DC distribution system with active stabilizer," *IEEE J. Emerg. Sel. Topics Power Electron.*, vol. 4, no. 1, pp. 93–102, Mar. 2016.
- [21] P. Magne, B. Nahid-Mobarakeh, and S. Pierfederici, "Active stabilization of DC microgrids without remote sensors for more electric aircraft," *IEEE Trans. Ind. Appl.*, vol. 49, no. 5, pp. 2352–2360, Sep. 2013.
- [22] R. L. Boylestad and L. Nashelsky, *Electronic Devices and Circuit Theory*, 10th ed. Upper Saddle River, NJ, USA: Prentice Hall, 2008.
- [23] A. Sahai and S. Mitter, "The necessity and sufficiency of anytime capacity for stabilization of a linear system over a noisy communication link-Part I: Scalar systems," *IEEE Trans. Inf. Theory*, vol. 52, no. 8, pp. 3369–3395, Aug. 2006.
- [24] S. ten Brink and G. Kramer, "Design of repeat-accumulate codes for iterative detection and decoding," *IEEE Trans. Signal Process.*, vol. 51, no. 11, pp. 2764–2772, Nov. 2003.
- [25] M. Noor-A-Rahim, M. O. Khyam, Y. L. Guan, G. G. M. Nawaz Ali, K. D. Nguyen, and G. Lechner, "Delay-universal channel coding with feedback," *IEEE Access*, vol. 6, pp. 37 918–37 931, 2018.
- [26] M. Noor-A-Rahim, K. D. Nguyen, and G. Lechner, "Finite length analysis of LDPC codes," in *Proc. IEEE Wireless Commun. Netw. Conf.*, 2014, pp. 206–211.
- [27] Sae-Young Chung, T. J. Richardson, R. L. Urbanke, S.-Y. Chung, T. J. Richardson, and R. L. Urbanke, "Analysis of sum-product decoding of low-density parity-check codes using a Gaussian approximation," *IEEE Trans. Inf. Theory*, vol. 47, no. 2, pp. 657–670, Feb. 2001.



Mohammad Omar Khyam received the Ph.D. degree in electrical engineering from the University of New South Wales, Sydney, Australia, in 2015.

He worked as a Postdoctoral Research Fellow with the National University of Singapore, Singapore, from 2016 to 2017, and Virginia Tech, Blacksburg, VA, USA, from 2018 to 2019. He is currently working as a Lecturer with Central Queensland University, Rockhampton, Australia. His current research interests include signal processing, wireless communication, machine learning, and robotics.



Md. Apel Mahmud (Senior Member, IEEE) received bachelor's degree in electrical engineering with from the Rajshahi University of Engineering and Technology, Rajshahi, Bangladesh, in 2008, and the Ph.D. degree in electrical engineering from the University of New South Wales, Sydney, Australia, in 2012.

He is currently working as a Senior Lecturer in electrical & renewable energy engineering with Deakin University, Geelong, Australia. He has also worked as a Lecturer in electrical & electronic engineering with Deakin University and Swinburne University of Technology, as a Research Fellow with the University of Melbourne, and as a Research Publication Fellow with the University of New South Wales. His research interests include power system stability, control of power systems including renewable energy sources as well as microgrids, energy management for microgrids, energy storage systems, transactive energy (data analytics), and nonlinear control theory.

Dr. Mahmud was the recipient of the Best Thesis Award from the University of New South Wales, in 2012.



Md. Tanvir Ishtaique ul Huque received the master's degree in electrical engineering from the University of Sydney, Canberra, Australia, in 2014, and the Ph.D. degree in electrical engineering from the University of New South Wales (UNSW), Sydney, Australia, in 2019.

He is a Research Fellow in cybersecurity with Queensland University of Technology, Brisbane, Australia. He was with the UNSW, Canberra, Data61-CSIRO, Sydney, and the University of Helsinki, Helsinki, Finland. He is actively working on projects

of critical infrastructure security.



Md. Noor-A-Rahim received the Ph.D. degree from the Institute for Telecommunications Research, University of South Australia, Adelaide, Australia, in 2015.

He was a Postdoctoral Research Fellow with the Centre for Infocomm Technology, Nanyang Technological University, Singapore. He is currently a Senior Postdoctoral Researcher (MSCA Fellow) with the School of Computer Science & IT, University College Cork, Cork, Ireland. His research interests include control over wireless networks, intelligent

transportation systems, machine learning, signal processing, and DNA-based data storage.

Dr. Noor-A-Rahim was the recipient of the Michael Miller Medal from the Institute for Telecommunications Research, University of South Australia, for the most Outstanding Ph.D. Thesis in 2015.



Xinde Li (Senior Member, IEEE) received the Ph.D. degree in control theory and control engineering from the Huazhong University of Science and Technology, Wuhan, China, in 2007.

After Ph.D., he joined the School of Automation, Southeast University, Nanjing, China, where he is currently a Professor and Ph.D. Supervisor. From 2012 to 2013, he was a Visiting Scholar with the School of Interactive Computing, Georgia Institute of Technology. In 2016, he was a Postdoc Research Fellow with the Department of Electrical and Computer

Engineering, National University of Singapore. His research interests include information fusion, object recognition, computer vision, intelligent robot, and human–robot interaction.

Dr. Li was the recipient of the Talent of Qing Lan Project Award of Jiangsu province and a Six Major Top-Talent Plan Award of Jiangsu province, China.



Dirk Pesch (Senior Member, IEEE) received the Dipl. Ing. degree from RWTH Aachen University, Aachen, Germany, and the Ph.D. degree from the University of Strathclyde, Glasgow, Scotland.

He is a Professor with the School of Computer Science and Information Technology, University College Cork, Cork, Ireland, and was previously the Head with the Nimbus Research Centre, Cork Institute of Technology. He has more than 25 years research and development experience in both industry and academia and has (co-)authored more than 200 scientific articles

and book chapters. He is a Principle Investigator of the National Science Foundation Ireland funded collaborative centres CONNECT (Future Networks) and CONFIRM (Smart Manufacturing), and the Director of the SFI Centre for Research Training in Advanced Networks for Sustainable Societies. He has also been involved in a number of EU funded research projects on smart and energy efficient buildings and urban neighborhoods, including as a Coordinator. His research interests include problems associated with architecture, design, algorithms, and performance evaluation of low power, dense, and vehicular wireless/mobile networks and services for Internet of Things and cyberphysical system's applications in building management, smart connected communities, independent living, and smart manufacturing.

Dr. Pesch serves as the Technical Programme Chair of the IEEE International Symposium on a World of Wireless, Mobile and Multimedia Networks 2020 and the Executive Vice-Chair of IEEE International Conference on Communications 2020.



Amanullah M. T. Oo (Senior Member, IEEE) is currently the Dean and the Head of the School of Engineering, Deakin University, Geelong, Australia. He is a Professor of electrical eEngineering and has made significant research contributions in the area of electrical power engineering and renewable energy, engineering education, and has authored and co-authored more than 250 scholarly articles in the peer reviewed high impact journals, books, and conference proceedings. He has supervised more than 15 Ph.D. students to completion and is currently supervising

several Ph.D. students in the area of electrical power engineering and renewable energy engineering. He has led Deakin University 30 million Microgrid research program. His research interests and expertise include microgrid & energy storage system integration, smart grid communication, power system stability and control, energy management and efficiency, protection and security of smart grids, sustainable operation and control of microgrids as well as in engineering education.

Prof. Maung has been actively working with several international and national professional communities and industries. He is sought worldwide to deliver keynote addresses and presentations at workshops and conferences.